

## Field Tests and Numerical Simulation of Thermal Response Test Equipment Applicable to Water Wells of Large Diameters

Satoshi Tanaka<sup>1</sup>, Hikari Fujii<sup>1</sup>, Hiroyuki Kosukegawa<sup>1</sup> and Retsu Harada<sup>2</sup>

<sup>1</sup> Graduate School of International Resource Sciences, Akita University, 1-1 Tegatagakuen-machi, Akita City, Akita, 010-8502, Japan

<sup>2</sup> BIOTEX Co., Ltd. 1853-3 Kubota-chou Tokuman, Saga City, Saga, 849-0201, Japan

fujii@mine.akita-u.ac.jp

**Keywords:** TRT, GHE, thermal conductivity, GSHP system, optical fiber thermometer

### ABSTRACT

This study aimed to validate the effectiveness of a novel TRT equipment applicable to large diameter water wells. The equipment consisted of an optical fiber thermometer, a cable heater, and cylindrical electromagnets, which heat the surrounding ground in close contact with the casing of the water well. The vertical distribution of apparent thermal conductivities of ground ( $\lambda_s$ ) is estimated by applying Kelvin's line source theory to temperature changes during the heating and recovery periods. First, TRTs were conducted four times with different heating periods using the new TRT equipment in a water well (204.7 mm ID) cased with steel pipes to investigate the necessary length of the heating period. The heating periods were changed from 0.5 days to 4 days, and the heat load of the heater was set to approximately 43 W/m for all four TRTs. Thereafter, estimated  $\lambda_s$  profiles were compared with a reference profile estimated from TRTs using cable heating method in the same test field. The  $\lambda_s$  profiles estimated from the heating periods of each test differed significantly from the reference profile due to the natural convection of groundwater around the well and the difference in the positional relationship between the heater and temperature sensor at each depth. In contrast, the  $\lambda_s$  profiles estimated from the recovery period showed good agreement with the reference profile when a heating period over 2 days was applied. Subsequently, the numerical models were developed using FEFLOW ver. 7.1 to reproduce the TRTs using the new TRT equipment. The heating periods required to estimate the appropriate  $\lambda_s$  profile were evaluated for larger well diameters of 300, 400, and 500 mm. The validity of the developed models was verified through the history matching of temperature changes. The simulation results showed a proportional relationship between the inner diameter of the wells and the required heating period, indicating that the new TRT equipment can be applied to large-diameter water wells by applying appropriate heating periods.

### 1. INTRODUCTION

The performance of ground source heat pump (GSHP) systems depends on the thermophysical properties of the ground, and thermal response tests (TRTs) are commonly conducted to determine apparent thermal conductivities of ground ( $\lambda_s$ ) and thermal resistance of ground heat exchangers (GHEs) for optimum design of GSHP systems. Conventional TRTs are conducted by circulating a heat medium through a U-tube inserted into a GHE under constant heat load and heating the ground surrounding the GHE. Thus, the implementation of conventional TRTs requires the drilling of GHEs and is costly and time-consuming. In particular, drilling costs are high in Japan owing to the complex geological structures and labor costs, which is one of the factors hindering the widespread use of GSHP systems. This study aimed to validate the effectiveness of a novel TRT equipment using cable heating that is applicable to existing water wells with large diameters instead of GHEs. TRTs applied to existing water wells can be implemented at lower costs and in a shorter time than conventional TRTs using GHEs because no new wells need to be drilled. TRTs can be implemented in existing water wells, such as pumping wells, snowmelt wells, and observation wells for groundwater using the new TRT equipment, and expansion of the database for the utilization of the GSHP system is also expected. Several TRT methods to estimate vertical  $\lambda_s$  profiles using heating cables have been proposed for cost and time reduction so far. Raymond et al. (2015) installed ten short heating cables in the pipe of a heat exchanger to inject heat and estimate the distribution of subsurface thermal conductivity. Isabel et al. (2018) conducted distributed thermal response tests (DTRT) using a heating cable and fiber-optic temperature sensor and attempted to obtain the thermal conductivity distribution. Zhang et al. (2020) conducted an actively heated fiber optics-based TRT (ATRT) and obtained a reliable thermal conductivity distribution through a comparison with the results of a conventional TRT. A copper-mesh-heated optical cable was used in the ATRT as a heating source, along with a temperature-sensing cable. Hakala et al. (2022) presented an enhanced thermal response test (ETRT) using a hybrid cable containing copper wires and fiber optics and determined the vertical distributions of thermal conductivities along the drill hole. TRT methods using cable heating for estimating the distribution of  $\lambda_s$  were summarized by Raymond et al. (2021). These attempts showed the effectiveness of TRTs using heating cables for  $\lambda_s$  estimation. However, no studies have been conducted on the application of TRT using heating cables in existing water wells with large diameters. Over the last few years, we have attempted to develop new TRT equipment applicable to existing water wells. Tanaka et al. (2022) proposed new TRT equipment consisting of electromagnets, a cable heater, and an optical fiber thermometer and conducted TRTs using the equipment in a water well cased with a steel pipe (150 mm ID) located at Akita University, Japan. The heating period and section were 4 h and 10 m, respectively. The equipment functioned correctly, and a heater and thermometer were attached to the casing using electromagnets during the tests. However, the estimated  $\lambda_s$  profile did not match the reference  $\lambda_s$  profile estimated from conventional TRTs conducted in the same well and interpreted using the analysis method proposed by Fujii et al. (2009). Subsequently, we developed a numerical model reproducing the TRT using the new equipment in FEFLOW ver. 7.1 and conducted case studies to estimate the appropriate  $\lambda_s$  profile. From the

results of the numerical simulations, the shortage of a heating period and heating section was a factor preventing the estimation of an appropriate thermal conductivity profile. In this study, we improved the new TRT equipment by extending the heating section to 40 m and the heating period to 4 days. In addition, temperature changes during the recovery period and the heating period were measured to estimate  $\lambda_s$  profiles from both periods, and results were compared with the reference profile.

## 2. INFORMATION OF TRT AND THE NEW TRT EQUIPMENT

### 2.1 Test field

The test field was located in Saga City, Kyushu, Japan (Figure 1 (a)), and the terrain was classified as an alluvial plain. Two experimental wells were drilled in the field in April 2023. Schematics of these wells are shown in Figure 1 (b). The first well was a GHE with a 25 A U-tube and backfilled with silica sand. The second well is a water well cased with a steel pipe (SGP, 200A) with an inner diameter of 204.7 mm and a pipe thickness of 5.8 mm. The hole size of the water well was 273.1 mm, and the space between the borehole and the casing was filled with silica sand. The depth of both wells was 50 m, and the separation distance was 1 m. The geological structure of the test field consists of alternating clay and sand layers, as shown in Figure 1 (c). The groundwater level was approximately -1 m below the ground surface.

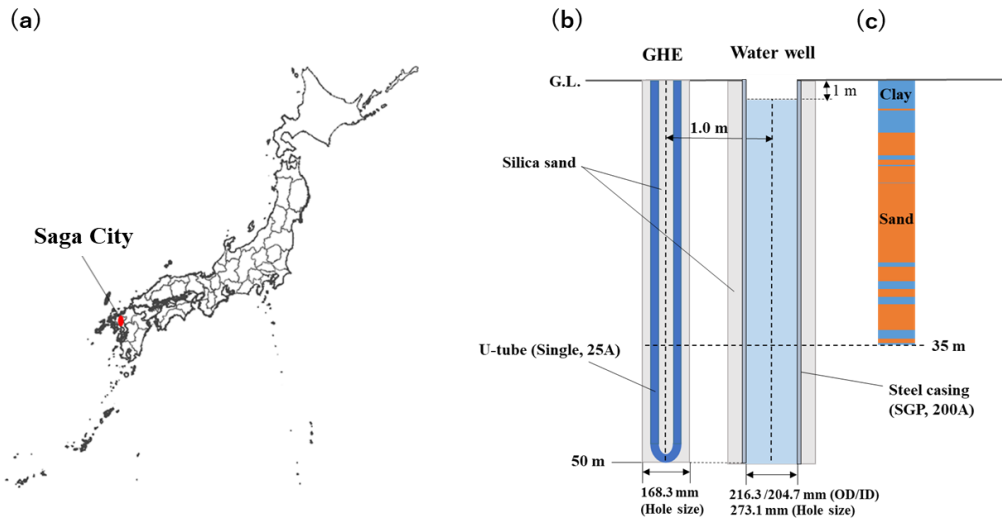


**Figure 1: (a) Location of the test field. (b) Schematics of the GHE and water well. (c) Geological column of the test field.**

### 2.2 New TRT equipment

The new TRT equipment was composed of a control unit and a measurement cable installed in the water well. The measurement cable comprised three main parts: a waterproof cable heater, an optical fiber thermometer, and cylindrical electromagnets. Figure 2 (a) shows the structure of the measurement cable and a photograph of the cable endpoint. The electromagnets did not exhibit adsorption directivity and were integrated into the measurement cable at intervals of 20 m, as shown in Figure 2 (a). The electromagnets adhered to the casing by passing an electrical current from the control unit. This equipment was designed to be used in water wells cased with steel pipes instead of GHEs, and the measurement cable was fixed on the steel casing using the electromagnets during the TRT. Figure 2 (b) shows a schematic of the TRT using the new TRT equipment in a water well. During the TRT, the ground around the water well is heated by the cable heater, and water temperatures are measured at 1.0 m intervals by the optical fiber thermometer to estimate  $\lambda_s$  at each depth as a vertical  $\lambda_s$  profile by applying the graphical method. The  $\lambda_s$  at each depth are estimated from the slope of the straight line of temperature change in the heating and recovery periods plotted in the semi-log graph of elapsed time vs temperature using Equation (1).

$$\lambda_s = 0.183q/m \quad (1)$$

where  $\lambda_s$ ,  $q$ ,  $m$  are the thermal conductivity of the ground (W/m/K), heat load per heating length (W/m), and slope of a straight line (K/cycle), respectively.

For the estimation of  $\lambda_s$  at each depth during recovery periods, Horner time ( $t_h$ ) is applied to the graphical method. Horner time is defined as Equation (2). The slope of the straight line of semi-log plots of Horner time vs temperature during recovery periods is used in Equation (1) to estimate  $\lambda_s$  at each depth. The interpretation method applied to the Horner plot for the recovery periods is explained by Fujii et al. (2002).

$$t_h = (\Delta t + t_f) / \Delta t \quad (2)$$

where  $t_h$ ,  $\Delta t$ ,  $t_f$ , are Horner time (-), elapsed time after the end of heating, and heating time, respectively.

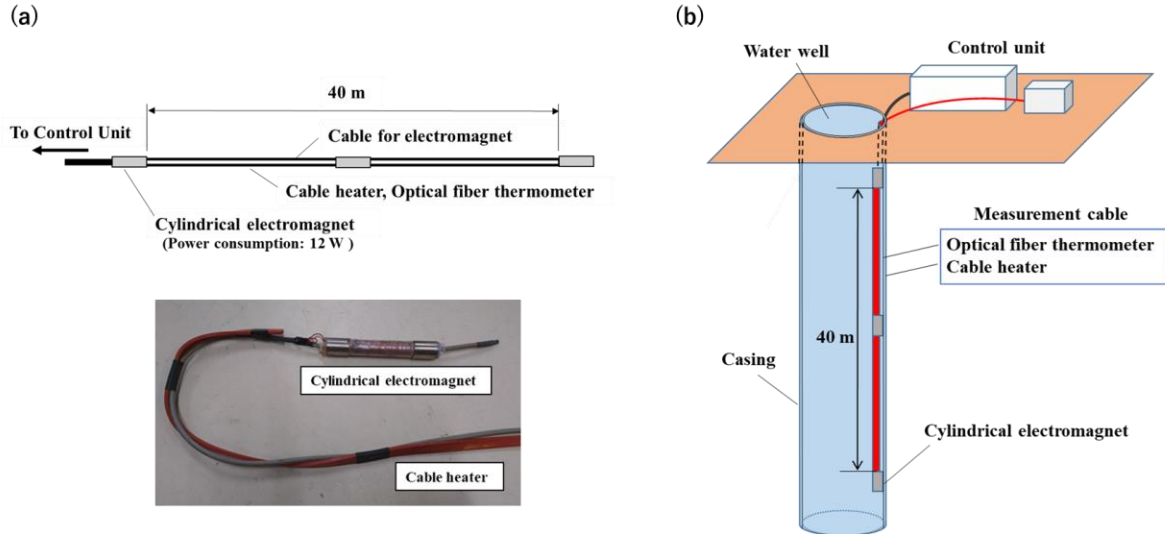


**Figure 2: (a) Structure of the measurement cable and a photograph of the endpoint of the cable. (b) Schematic of the TRT using the new TRT equipment in the water well.**

### 3. TRT CONDITIONS

In this study, four TRTs were conducted in the test field. TRTs were conducted as TRT 1-a, 1-b, 1-c, and 1-d using the new TRT equipment in the water well to validate the effectiveness of the equipment by comparing estimated  $\lambda_s$  profiles with a reference profile. The reference  $\lambda_s$  profile was estimated from TRTs using the cable heating method conducted by Fujii et. al (2024) in the GHE adjacent to the water well, as shown in Figure 3 (a). Table 1 lists the names and conditions for each TRT. Figure 3 (b) shows a schematic of TRT 1-a, 1-b, 1-c and 1-d. In these tests, different heating periods from 0.5 days to 4.0 days were applied for each test under a fixed heat load of around 43 W/m to evaluate the heating periods required to estimate the appropriate  $\lambda_s$  profile. The temperature recovery periods after heating were set from 1.1 days to 4 days, depending on the heating period of each test. Before the TRTs were conducted in the water well, the internal condition of the well was checked using a borehole camera, and mud accumulation was confirmed at a depth of 45 m. Thus, the measurement cable was installed at depths ranging from 5 to 45 m on the casing to avoid mud accumulation. After installing the measurement cable, the inside condition of the well was checked again using a borehole camera, and the measurement cable was in good contact with the casing. Temperature changes at each depth during the heating and recovery periods were measured at 60-second intervals for all tests using an optical fiber thermometer.  $\lambda_s$  profiles for 5 m from the bottom of the optical fiber sensor were not calculated due to low data quality around the endpoint of the optical fiber. Figure 3 (c) shows a photograph of the TRT 1-d implementation.

**Table 1: Conditions of TRTs**

TRT number	Well type	Heat load (W/m)	Heating period (days)	Recovery period (days)	Depth of heating section (m)	Test date
TRT 1-a	Water well	42.7	0.5	1.1	5 - 45	2023/8/21-8/23
TRT 1-b	Water well	42.9	1.0	2.0	5 - 45	2023/9/1-9/4
TRT 1-c	Water well	43.8	2.0	2.0	5 - 45	2023/7/26-7/30
TRT 1-d	Water well	44.3	4.0	4.0	5 - 45	2023/7/6-7/14

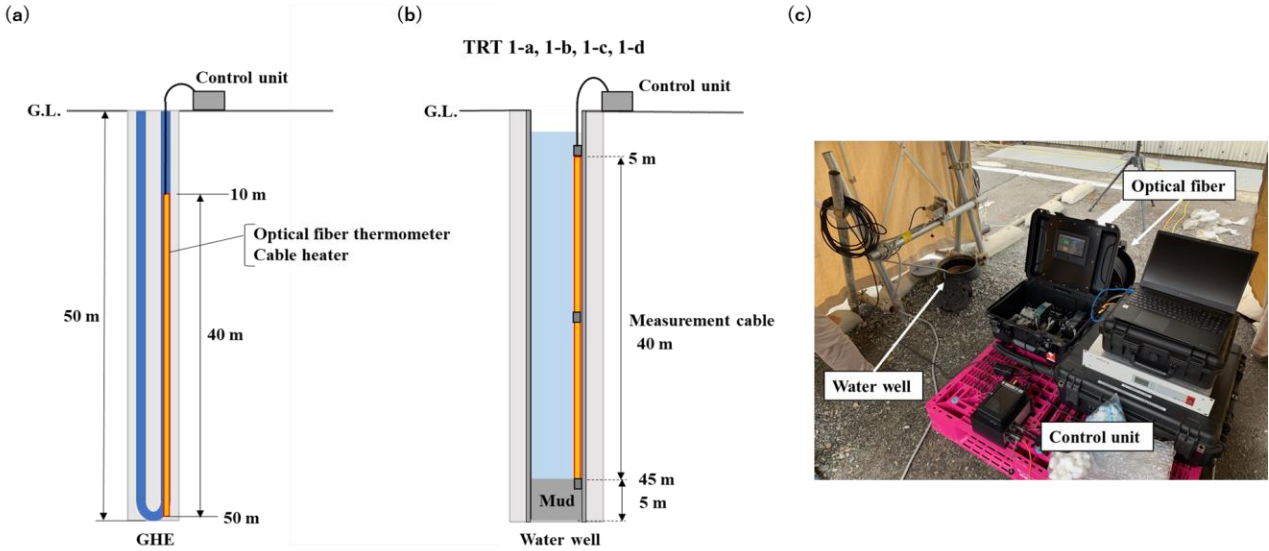


**Figure 3: (a) Schematics of TRTs in the GHE. (b) Schematics of TRTs in the water well (TRT 1-a, 1-b, 1-c and 1-d). (c) Photograph of TRT 1-d implementation.**

#### 4. RESULTS AND DISCUSSION OF TRTS

##### 4.1 Results of TRTs in the water well (TRT 1-a, 1-b, 1-c, 1-d)

In TRTs in the water well, the heating period was varied from 0.5 to 4 days to evaluate the heating period required to estimate the appropriate  $\lambda_s$  profile. The heat load of the heater was set at approximately 43 W/m to transfer enough heat to the ground around the well for the  $\lambda_s$  interpretation since some of the heat from the heater was used for heating the groundwater in the well with a large heat capacity. Figure 4 (a) and (b) show the temperature change at 10 m intervals in the measurement section for graphical interpretation during the heating and recovery periods of TRT 1-c, respectively. As shown in Figure 4 (a), straight lines were observed from 24 hours after the start of heating. In Figure 4 (b), straight lines were observed when the Horner time was less than 5, corresponding to approximately 12.2 hours or later after heating was stopped.  $\lambda_s$  profiles in TRT 1-c were estimated from the slopes of lines of each depth using the graphical method.  $\lambda_s$  profiles in TRT 1-a, 1-b, and 1-d were also estimated by applying the same interpretation method with TRT 1-c to the temperature changes during the heating and recovery periods. Figure 5 (a) shows  $\lambda_s$  profiles estimated from heating periods of TRT 1-a through 1-d, and Figure 5 (b) shows  $\lambda_s$  profiles estimated from recovery periods of TRT 1-a through 1-d. From Figure 5 (a),  $\lambda_s$  profiles estimated from heating periods of each TRT showed poor agreement with the reference profile. This is considered due to the natural convection of groundwater saturating the formation around the well and the difference in the positional relationship between the heater and the optical fiber thermometer at each depth. On the other hand, estimated  $\lambda_s$  profiles from the recovery periods of each TRT show better agreement with the reference profile and show the same trend, particularly from a depth of approximately 20 to 40 m. This could be attributed to the difference in the distance between the heater and optical fiber sensor did not affect the temperature changes at each depth during the recovery period, and the natural convection of groundwater in the formation did not occur during the recovery period. The estimated  $\lambda_s$  profiles in the depth from 10 m to 20 m show some difference from the reference profile, and this is caused by the heterogeneity of the geological structure between the GHE and the water well due to the high degree of geological complexity in this test field. Figure 6 shows the root mean square (RMS) errors between the  $\lambda_s$  profiles estimated from the recovery period of each TRT shown in Figure 5 (b) and the reference profile in the section from the depth of 10 m to 40 m. The RMS of the  $\lambda_s$  profiles estimated from the TRTs in the water well converged to approximately 0.35 W/m/K after 2 days or more heating period. From the above results, appropriate  $\lambda_s$  profile can be estimated using the new TRT equipment in water wells with around 200 mm ID or less by applying the heating period of over 2 days.

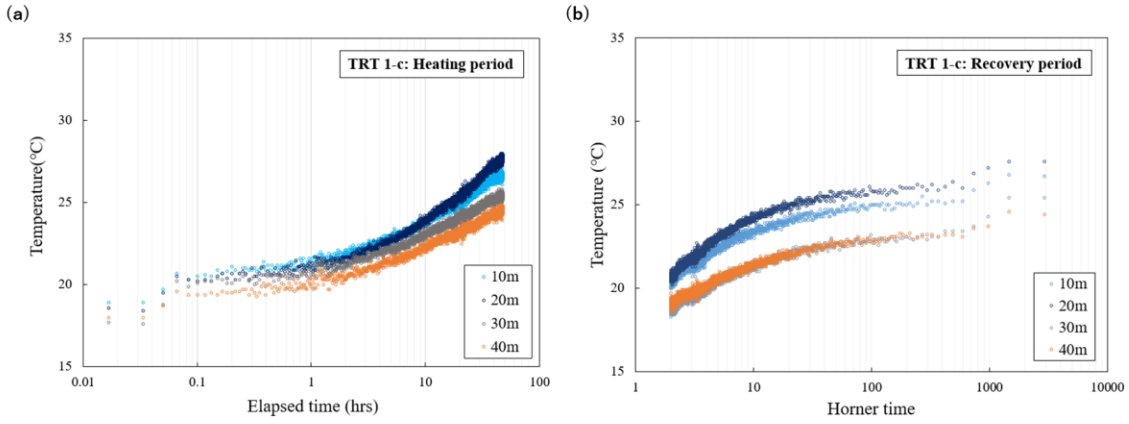


**Figure 4:** (a) Temperature changes at each depth during the heating period of TRT 1-c. (b) Temperature changes at each depth during the recovery period of TRT 1-c.

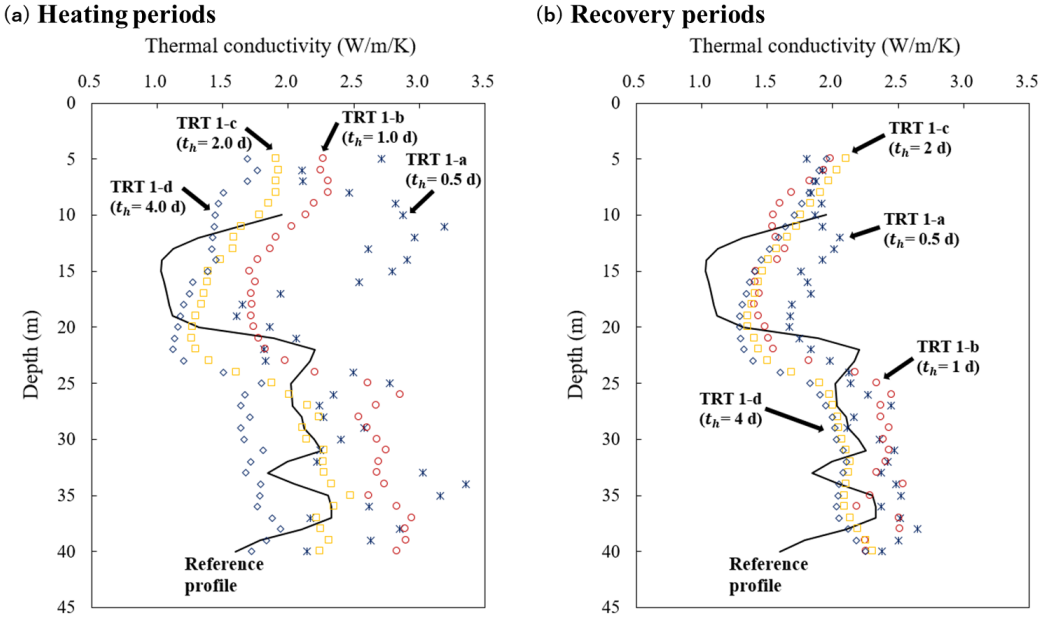


**Figure 5:** (a)  $\lambda_s$  profiles estimated from heating periods of TRT 1-a through 1-d. (b)  $\lambda_s$  profiles estimated from recovery periods of TRT 1-a through 1-d.

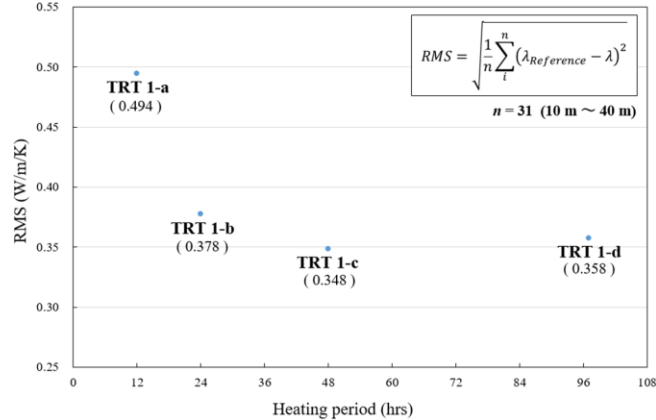


**Figure 6:** RMS errors between the  $\lambda_s$  profiles estimated from the recovery period of each TRT and the reference profile in the section from the depth of 10 m to 40 m.

## 5. DEVELOPMENT OF THE NUMERICAL MODEL

### 5.1 Information of the numerical model

A numerical model reproducing TRTs in the water well using the new TRT equipment was developed using FEFLOW ver. 7.1 for case studies to evaluate the effect of well diameters for estimation of  $\lambda_s$  profiles. Figure 7 (a) and (b) show a cross-sectional view of the developed numerical model in the X-Y plane and a 3D view of the model, respectively. In the model, the water well was positioned at the center of a square ground with a length of 6.0 meters on each side. The height of the model was 60 m, and it comprised 60 layers. The dimensions of the well for TRTs were set to 204.7 mm ID with a pipe thickness of 5.8 mm, as the actual well used for TRT 2-a to 2-d. The thermal conductivities in the ground area at each depth were input thermal conductivity values of the reference  $\lambda_s$  profile for each layer. The heat generated by the heater was reproduced by inputting heat fluxes from depths of 5 m to 45 m, and the external boundary of the model was set as the adiabatic condition.

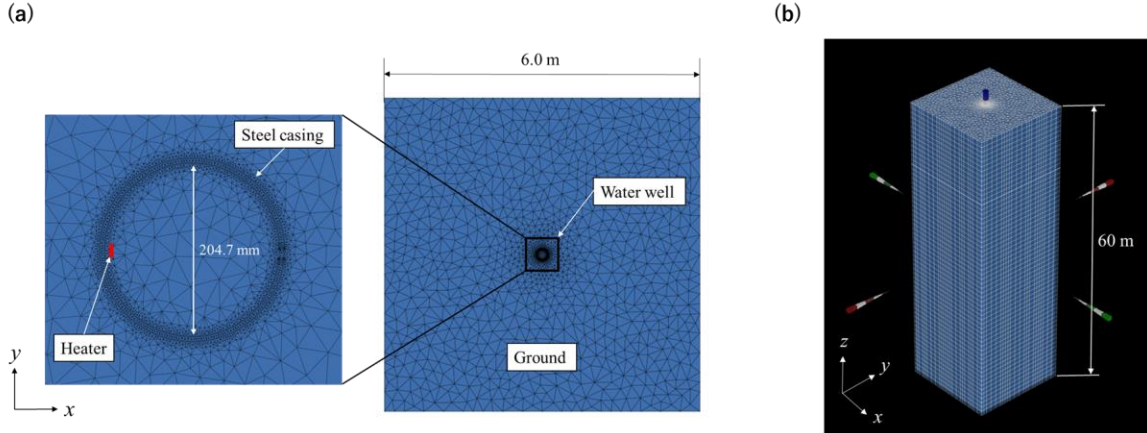


**Figure 7: (a) A cross-sectional view of the numerical model in the X-Y plane. (b) 3D view of the model.**

### 5.2 Results of history matchings

A numerical simulation reproducing TRT 2-c was conducted using the developed model to verify its validity through history matching. The initial temperature and heat load of the heater in the model were set to 18.4°C and 43.8 W/m, respectively, based on the test data of TRT 2-c. The heating and recovery periods were set to 2.0 days, and history matchings of temperature changes during both periods were performed at each depth in the measurement section. Figure 8 shows the results of history matching at depths of 15, 25, and 35 m as a representative during the heating period. Similarly, Figure 9 shows the results of history matching at depths of 15, 25, and 35 m as a representative during the recovery period. As shown in Figures 8 and 9, the historical matches of the temperature changes at each depth in both the heating and recovery periods showed good agreement. Thus, the validity of the developed numerical model was confirmed through history matching.

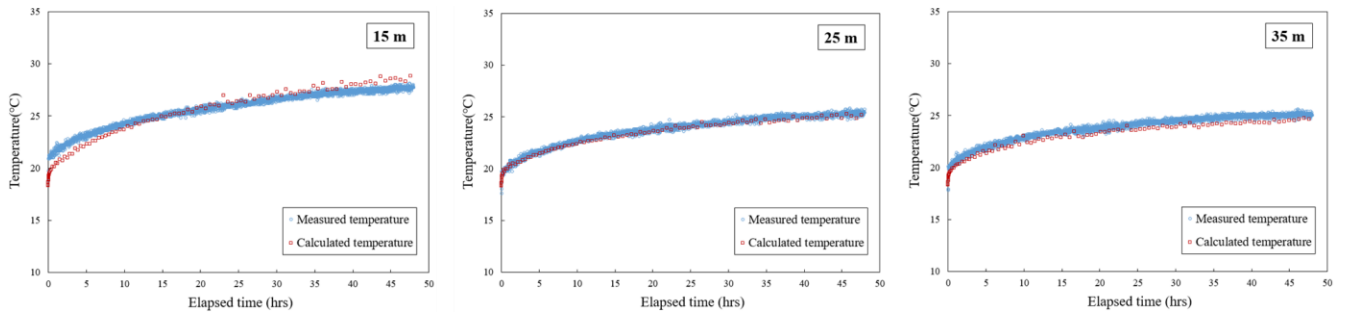


**Figure 8: Results of history matchings at depths of 15 m, 25 m, and 35 m during the heating period.**

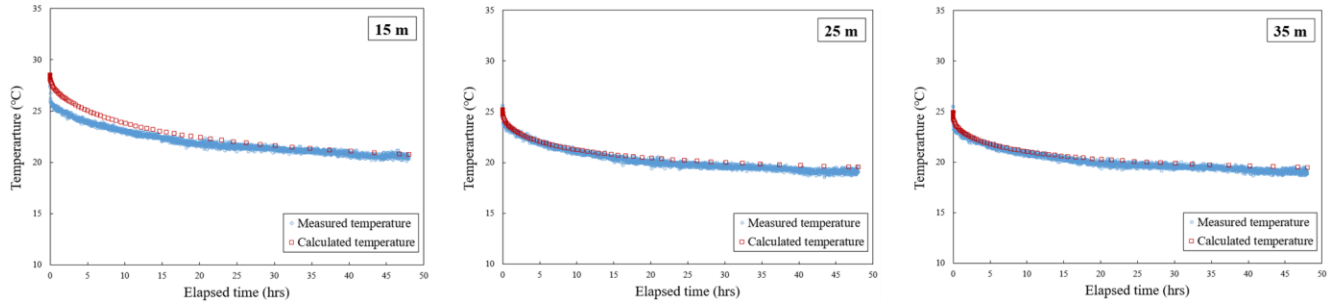


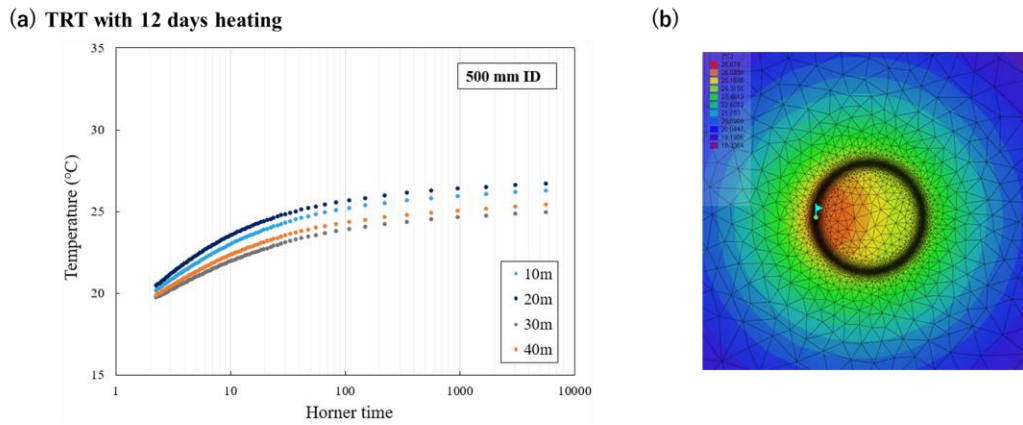
**Figure 9: Results of history matchings at depths of 15 m, 25 m, and 35 m during the recovery period.**

## 6. CONDITIONS OF CASE STUDIES

Numerical models were developed to simulate TRTs using the new TRT equipment in water wells with inner diameters of 300 mm, 400 mm, and 500 mm based on the model validated by history matchings, and case studies were conducted to evaluate heating periods for each well size required to estimate appropriate  $\lambda_s$  profiles. A maximum heating period of 10 days was set for TRTs in the well with 300 mm ID, and 12 days for 400 mm ID and 500 mm ID. The temperature recovery period in each TRT simulation case was set to be the same as the heating period. The heat load of the heater was set to 43.8 W/m for all TRT simulations, and the heating section was input to a depth of 5- 45 m, corresponding to the TRTs conducted in the water well.

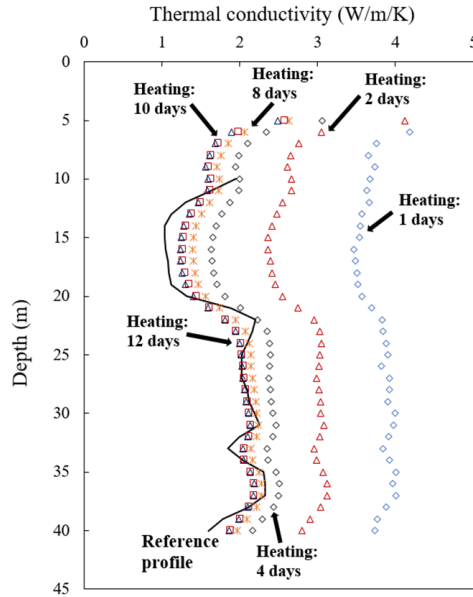
## 7. RESULTS AND DISCUSSION OF CASE STUDIES

Figure 10 (a) shows the temperature change at 10 m intervals for graphical interpretation during the recovery period of the TRT simulated 12 days of heating in the well with a 500 mm ID. Figure 10 (b) shows the temperature distribution at a depth of 20 m, 12 days after the start of heating. Groundwater in the well was not uniformly heated 12 days after the start of heating because of the large volume of groundwater in the well, as shown in Figure 10 (b); however, sufficient heat transfer to the ground around the well could be confirmed. In Figure 10 (a), straight lines at each depth were observed when the Horner time was less than 4, corresponding to approximately 4.1 days or later after the heating was stopped. The  $\lambda_s$  profile for the TRT of 12 days of heating in the well with 500 mm ID was estimated by applying the graphical method to the slope of the straight line of each depth. The same interpretation method was applied to the temperature changes during the recovery periods of TRTs simulated with other heating periods in wells with 500 mm ID, and estimated  $\lambda_s$  profiles are shown in Figure 11 (a). The difference between the estimated profiles from the TRT simulations and the reference profile decreased when the heating period was extended. Figure 11 (b) shows the RMS errors between the  $\lambda_s$  profiles estimated from the recovery period of each TRT simulation shown in Figure 11 (a) and the reference profile in the section from the depth of 10 m to 40 m. The RMS of the  $\lambda_s$  profiles estimated from the simulated TRTs in the well with 500 mm ID converged to approximately 0.20 W/m/K after around 10 days or more heating period. The results of these case studies indicate that water wells with 500 mm ID need a heating period five times longer than wells with approximately 200 mm ID to estimate appropriate profiles. This is considered due to the most of heat emitted from the heater being spent for heating groundwater in the well and it takes a longer period to heat the ground around the well sufficiently for  $\lambda_s$  interpretation compared with the TRTs in the well of about 200 mm ID.



**Figure 10: (a) Temperature change at 10 m intervals for graphical interpretation during the recovery period of the TRT simulated 12 days heating in the well with 500mm ID. (b) Temperature distribution at a depth of 20 m at 12 days after the start of heating. (X-Y plane)**

(a) Water well with 500 mm ID



(b)

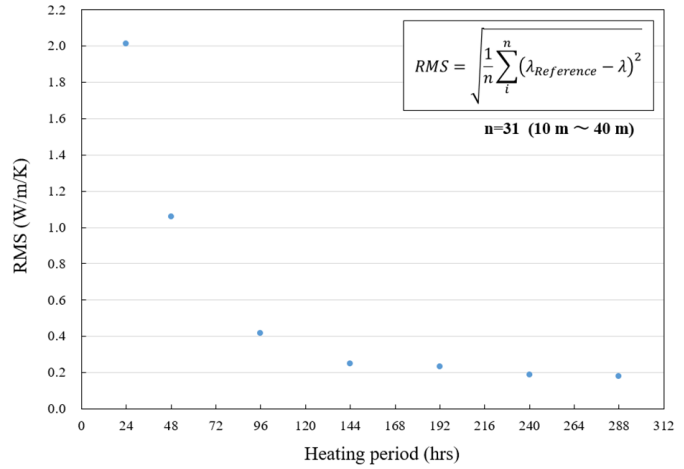
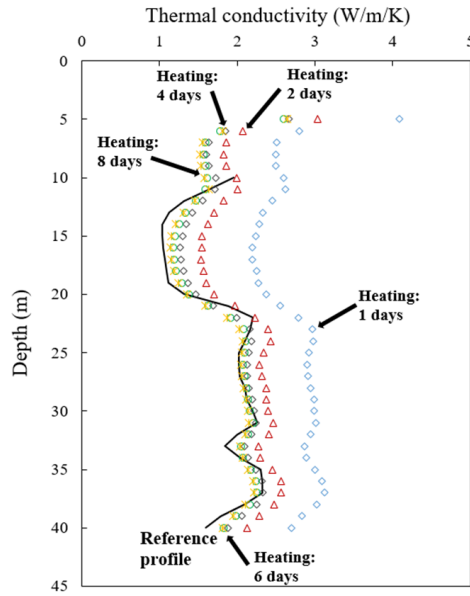


**Figure 11: (a)  $\lambda_s$  profiles estimated from the recovery periods of each TRT simulation conducted with different heating periods in the well with 500 mm ID. (b) RMS errors between the  $\lambda_s$  profiles estimated from the recovery period of each TRT simulation in the well with 500 mm ID and the reference profile.**

TRTs with different heating periods in the well of 300 mm and 400 mm ID were simulated, and  $\lambda_s$  profiles of each case were estimated to evaluate the required heating periods for each well size using the same interpretation method applied to the TRT simulations of the well with 500 mm ID. Figure 12 (a) shows  $\lambda_s$  profiles estimated from the recovery periods of each TRT simulation conducted with different heating periods from 1 to 8 days in the well with 300 mm ID, and Figure 12 (b) shows RMS errors between the  $\lambda_s$  profiles estimated from the recovery periods of each TRT simulation in the well with 300 mm ID and the reference profile. Similarly, Figure 13 (a) shows  $\lambda_s$  profiles estimated from recovery periods of each TRT simulation conducted with different heating periods from 1 to 10 days in the well with 400 mm ID, and Figure 13 (b) shows RMS errors between the  $\lambda_s$  profiles estimated from the recovery periods of each TRT simulation in the well with 400 mm ID and the reference profile. From Figure 12 (b), The RMS of the  $\lambda_s$  profiles estimated from the TRT simulations in the well with 300 mm ID converged to around 0.15 W/m/K after around 5 days or more heating period. From Figure 13 (b), The RMS of the  $\lambda_s$  profiles estimated from the TRT simulations in the well with 400 mm ID converged to approximately 0.17 W/m/K after around 7 days or more heating period. From the results of case studies, at least around 5 days, 7 days, and 10 days of heating periods were required to estimate appropriate  $\lambda_s$  profile from TRTs in the water well with 300 mm, 400 mm, and 500 mm ID, respectively. The longer heating period is required to converge the estimated  $\lambda_s$  with increasing the inner diameter of water wells due to increase of volume of the groundwater in the well. Figure 14 shows the required heating periods for each inner diameter of the water wells, as indicated by the case studies and field tests. The inner diameter of the water well and the required heating period exhibited a proportional relationship. From the above results, the new TRT equipment can be applied to TRTs in water wells of large diameters to estimate  $\lambda_s$  profile by applying the appropriate heating periods depending on the inner diameter of the well, according to Figure 14.

(a) Water well with 300 mm ID



(b)

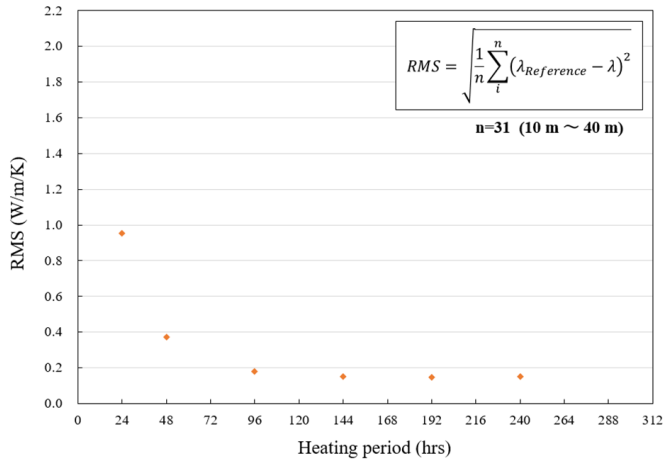
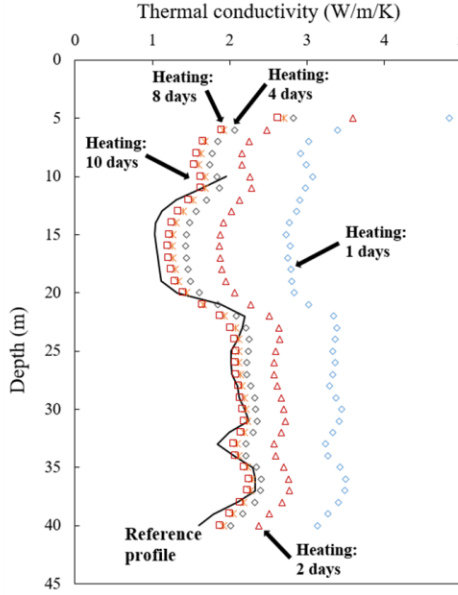


Figure 12: (a)  $\lambda_s$  profiles estimated from the recovery periods of each TRT simulation conducted with different heating periods in the well with 300 mm ID. (b) RMS errors between the  $\lambda_s$  profiles estimated from the recovery period of each TRT simulation in the well with 300 mm ID and the reference profile.

(a) Water well with 400 mm ID



(b)

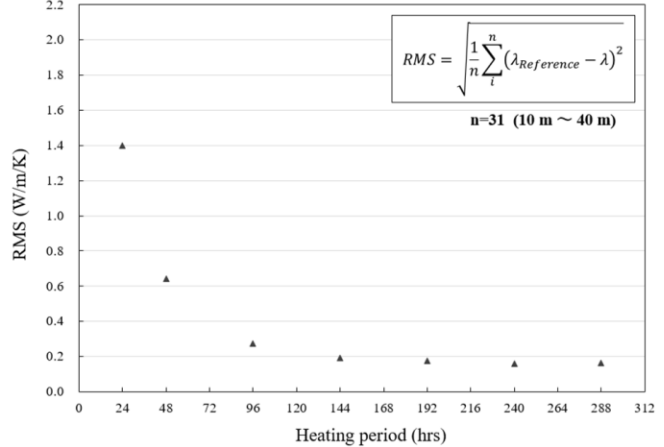
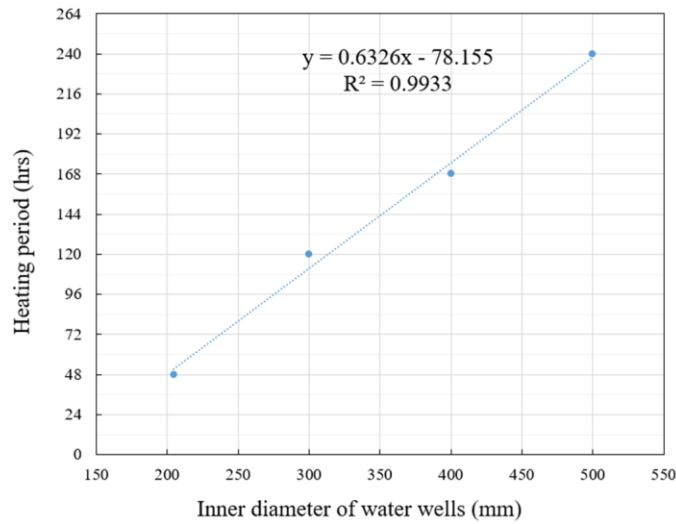


Figure 13: (a)  $\lambda_s$  profiles estimated from the recovery periods of each TRT simulation conducted with different heating periods in the well with 400 mm ID. (b) RMS errors between the  $\lambda_s$  profiles estimated from the recovery period of each TRT simulation in the well with 400 mm ID and the reference profile.



**Figure 14: Required heating periods for each inner diameter of water wells.**

## 8. CONCLUSIONS

In this study, the effectiveness of a novel TRT equipment applicable to water wells of large diameters was validated through TRTs conducted in the test field and case studies using numerical models. The equipment consisted of a control unit and a measurement cable comprising a cable heater, an optical fiber thermometer, and cylindrical electromagnets. The cable was attached to the steel casing of the water wells using electromagnets during the TRT, and the ground around the well was heated by the cable heater.  $\lambda_s$  profiles are estimated from the measured temperature at each depth in the heating section by applying the graphical method based on Kelvin's line source theory. Four TRTs using the new TRT equipment were conducted in a water well with 204.7 mm ID drilled in Saga City, Japan. Temperature changes during the heating and recovery periods were measured for all TRTs, and  $\lambda_s$  profiles were estimated from both periods. TRTs were conducted by changing heating periods from 0.5 days to 4 days under a heat load of around 43 W/m, and required heating periods to estimate appropriate  $\lambda_s$  profile were evaluated. From the results of four TRTs,  $\lambda_s$  profiles estimated from heating periods showed significant differences with the reference profile due to the difference in the positional relationship between the heater and optical fiber thermometer at each depth and the effect of the natural convection of groundwater in the formation. On the other hand,  $\lambda_s$  profiles estimated from recovery periods showed better agreement and the same trend with the reference profile, and indicated the appropriate  $\lambda_s$  profiles can be estimated from temperature change during recovery periods by applying heating periods of 2 days or more. Thereafter, case studies were conducted using numerical models to evaluate the heating periods required for TRTs in wells with larger inner diameters. A numerical model was developed using the FEFLOW ver. 7.1. The validity of the model was confirmed by the history matching of the temperature changes at each depth during both the heating and recovery periods. Numerical models to simulate TRTs using the new TRT equipment in water wells with 300 mm, 400 mm, and 500 mm ID were developed based on the validated model, and required heating periods to estimate appropriate  $\lambda_s$  profiles from recovery periods were investigated for each well size under a heat load of 43.8 W/m. From the results of case studies, at least approximately 5 days, 7 days, and 10 days heating periods were required for the estimation of appropriate  $\lambda_s$  profile from TRTs in the water well with 300 mm, 400 mm, and 500 mm ID, respectively. Thus, the inner diameter of the water well and the required heating period to estimate the  $\lambda_s$  profile showed a proportional relationship. In conclusion, the new TRT equipment can be applied to TRTs in water wells of large diameters to estimate  $\lambda_s$  profile by applying the appropriate heating periods depending on the inner diameter of the well.

## ACKNOWLEDGMENT

This paper is based on results obtained from a project, JPNP19006, subsidized by the New Energy and Industrial Technology Development Organization (NEDO).

## REFERENCES

Fujii, H., S., Akibayashi, K., Ohshima.: Interpretation of Thermal Response Tests in Shallow Deposits, Geothermal Resources Council Transactions, 26, (2002), 143-148.

Fujii, H., H, Okubo., K, Nishi., R, Itoi., K, Ohyama and K, Shibata.: An improved thermal response test for U-tube ground heat exchanger based on optical fiber thermometers, Geothermics, 38, (2009), 399-406.

Fujii, H., S, Tanaka., H, Kosukegawa and R, Harada.: Development of thermal response test equipment applicable to water wells of large diameters, Proceedings, IGSHPA Research Track, (2024). (in press)

Hakala, P., S, Vallin., T, Arola., and I, Martinkauppi.: Novel use of the enhanced thermal response test in crystalline bedrock, Renewable Energy, 182, (2022), 467-482.

Isabel, M., V, Márquez., J, Raymond., D, Blessent., M, Philippe., N, Simon., O, Bour and L, Lamarche.: Distributed Thermal Response Tests Using a Heating Cable and Fiber Optic Temperature Sensing. *Energies*, 11, (2018), 3059.

Raymond, J., L, Lamarche and M, Malo.: Field demonstration of a first thermal response test with a low power source, *Applied Energy*, 147, (2015), 30-39.

Raymond, J., Maria, I. V. M., Daniela, B., Louis, L., Louis, G., Jean, R., Mikael, P., René, T., and Michel, Malo.: Ten Years of Thermal Response Test with Heating Cables, *Proceedings, World Geothermal Congress 2020+1*, Reykjavik, Iceland, October (2021).

Tanaka, S., H., Fujii, H., Kosukegawa, S., Tsuya.: Field tests and numerical simulation of a novel thermal response test equipment for water wells, *Proceedings, IGSHPA Research Track*, Las Vegas, (2022), 104-111.

Zhang, B., K, Gu., B, Shi., C, Liu., P, Bayer., G, Wei., X, Gong and L, Yang.: Actively heated fiber optics based thermal response test: A field demonstration. *Renewable and Sustainable Energy Reviews*, 134, (2020), 110336.